Cell, Vol. 120, 761–772, March 25, 2005, Copyright ©2005 by Elsevier Inc. DOI 10.1016/j.cell.2005.01.009

The Birnavirus Crystal Structure Reveals Structural Relationships among Icosahedral Viruses

Fasséli Coulibaly,[1] Christophe Chevalier,[2] Irina Gutsche,[1] Joan Pous,[1] Jorge Navaza,[1] Stéphane Bressanelli,[1] Bernard Delmas,[2,*] and Félix A. Rey[1,*]

[1]Laboratoire de Virologie Moléculaire et Structurale
UMR 2472/1157 CNRS-INRA and IFR 115
1 Avenue de la Terrasse, 91198 Gif-sur-Yvette Cedex
[2]Unité de Virologie et Immunologie Moléculaires
INRA
Domaine de Vilvert, 78350 Jouy-en-Josas
France

Summary

Double-stranded RNA virions are transcriptionally competent icosahedral particles that must translocate across a lipid bilayer to function within the cytoplasm of the target cell. Birnaviruses are unique among dsRNA viruses as they have a single T = 13 icosahedral shell, lacking the characteristic inner capsid observed in the others. We determined the crystal structures of the T = 1 subviral particle (260 Å in diameter) and of the T = 13 intact virus particle (700 Å in diameter) of an avian birnavirus to 3 Å and 7 Å resolution, respectively. Our results show that VP2, the only component of the virus icosahedral capsid, is homologous both to the capsid protein of positive-strand RNA viruses, like the T = 3 nodaviruses, and to the T = 13 capsid protein of members of the *Reoviridae* family of dsRNA viruses. Together, these results provide important insights into the multiple functions of the birnavirus capsid and reveal unexpected structural relationships among icosahedral viruses.

Introduction

Birnaviruses form a distinct family of double-stranded RNA (dsRNA) viruses infecting animal species as different as vertebrates, mollusks, insects, and rotifers (Delmas et al., 2004). The virions are nonenveloped, icosahedral particles of triangulation T = 13 with a diameter of about 700 Å (Bottcher et al., 1997). Unlike other dsRNA viruses, certain birnavirus properties—their genomic arrangement and genome replication strategy—are shared with positive-strand RNA (+sRNA) viruses (Birghan et al., 2000). Most of the research efforts on birnaviruses have focused on the infectious bursal disease virus (Muller et al., 2003), which shows interesting virulence properties and is responsible for important losses in the poultry industry. Another economically important birnavirus is the infectious pancreatic necrosis virus (IPNV) of salmonids (Delmas et al., 2004).

Nonenveloped icosahedral RNA viruses can be classified in two major categories according to their genome type: +sRNA and dsRNA. Among +sRNA eukaryotic viruses, the building block of the capsid—the "coat protein"—exhibits a special fold, the "jelly roll" β barrel (Rossmann and Johnson, 1989). This protein forms a tightly closed protein shell protecting the viral RNA, with the jelly roll β barrel oriented such that the β strands run tangentially to the particle surface. Except for the very small satellite +sRNA viruses—in which the capsid contains only 60 copies of the coat protein—most virus capsids contain 60 copies of a multimer (Harrison, 2001b), organized in an icosahedral surface lattice following the rules of quasiequivalence (Caspar and Klug, 1962). Such an arrangement leads to alternating 5-fold (I5 for "icosahedral 5-fold") and quasi-6-fold (Q6) contacts among coat proteins, distributed according to the triangulation of the surface lattice (Johnson and Speir, 1997).

In contrast to the +sRNA viruses, the crystal structures of dsRNA virus particles revealed a characteristic icosahedral shell composed of 120 subunits of a large coat protein, with a 3D fold completely unrelated to the universal jelly roll described above (Harrison, 2001a). The corresponding surface lattice does not follow the quasiequivalence principle, the building block being an asymmetric dimer. The simplest dsRNA virus of known structure, L-A virus, an intracellular yeast totivirus (*Totiviridae* family), has a capsid organized in this way (Caston et al., 1997; Naitow et al., 2002).

Detailed structural data are available also for members of the *Reoviridae* family of dsRNA viruses (Grimes et al., 1998; Nakagawa et al., 2003; Reinisch et al., 2000), which have multishelled architectures. The innermost shell displays the same organization as that observed in the totivirus capsid, with 60 asymmetric coat protein dimers. This structure is surrounded by a second icosahedral protein shell of triangulation T = 13, i.e., organized according to the quasiequivalence principle. The subunit of this second layer is a protein folded in two different domains (termed "base" and "head") forming trimers that constitute the building blocks of the shell. The trimers are disposed as towers on top of the smooth inner shell, with the α-helical base domain making contacts both with the inner capsid and with adjacent trimers, leaving holes at the I5 and Q6 axes to make a "fenestrated" lattice sealed at the bottom by the inner capsid. The head domain is a β barrel with a jelly roll topology, but in this case it projects away from the particle surface, with the β strands running radially rather than tangentially, and is not involved in contacts between trimers in the lattice (Grimes et al., 1998; Liemann et al., 2002; Mathieu et al., 2001).

An important property of dsRNA viruses—in contrast to +sRNA viruses—is that the viral genome is maintained protected within the particles throughout the virus cycle. The particles themselves carry out several enzymatic activities necessary for replication, like transcription and mRNA capping, that are directed by specific enzymes contained within the virion (polymerase, methyl transferase, etc.). Such activities require that the

*Correspondence: rey@vms.cnrs-gif.fr (F.A.R.); delmas@jouy.inra.fr (B.D.)

particles be translocated across the cell membrane without disassembling during entry—or undergoing only partial disassembly.

Among the *Reoviridae* family, orthoreoviruses use their T = 13 layer for interactions with the cell membrane during entry, partially disassembling to release transcriptionally active core particles into the cytoplasm (Nibert and Schiff, 2001). Rotaviruses and orbiviruses (also members of the *Reoviridae* family) have a third icosahedral protein layer that is used for specific interactions with the host, resulting in the release of double-layered particles across the cell membrane into the cytoplasm (Estes, 2001; Roy, 2001). Totiviruses, which lack the additional shells, are special because they are not capable of infecting other cells and are thus only transmitted vertically, exclusively during cell division.

In addition, low-resolution electron microscopy (EM) studies of the dsRNA bacteriophage phi-6 (family *Cystoviridae*) suggested the presence of an internal capsid with the characteristic arrangement of 60 asymmetric dimers surrounded by a T = 13 protein layer, which is in turn enclosed within a lipid bilayer containing several other proteins (Butcher et al., 1997). The similar arrangement of *Cysto*-, *Reo*-, and *Totiviridae* has led to the assignment of a putative single viral lineage encompassing these three families of dsRNA viruses (Bamford et al., 2002).

EM studies of IBDV virions have shown that they lack the characteristic inner capsid present in all the other dsRNA viruses (Bottcher et al., 1997). The T = 13 icosahedral surface of the birnavirus particle features trimeric projections similar to those of the second layer of the *Reoviridae*, but the lattice is not fenestrated, suggesting that the coat protein has a domain responsible for sealing the interior of the virus in addition to the projecting domain. Like all the other dsRNA viruses, birnavirus particles have been shown to become transcriptionally active in the presence of nucleotides (Cohen, 1975; Spies et al., 1987), extruding nonpolyadenylated mRNAs through pores in the capsid. It is presently not known if these mRNAs are capped. The single-layered capsid architecture raises important questions concerning the particle translocation across the cell membrane for transcription.

The birnavirus genome is composed of two segments, one of them coding for the viral polymerase VP1 (which is covalently attached in the virion to the genomic RNA segments), and the other for the polyprotein precursor pVP2-VP4-VP3 and for a separate small protein, VP5, of unknown function. VP4 is a protease that cleaves its own N and C termini in the polyprotein, thus also releasing pVP2 and VP3 within the infected cell (Birghan et al., 2000). Subsequent serial cleavages at the C terminus of pVP2 yield the mature VP2 protein and four peptides that remain associated with the virion (Da Costa et al., 2002). A possible role for these peptides could be destabilization of the cell membrane during entry. Birnavirus particle morphogenesis was shown to be controlled by VP3, which interacts both with the C-terminal end of the precursor pVP2 and with VP1 (Chevalier et al., 2004; Ona et al., 2004). The sequential maturation of pVP2 to VP2 takes place only upon particle assembly (Chevalier et al., 2002). Expression of VP2 by itself leads to dodecahedral T = 1 subviral particles (SVP) containing 20 VP2 trimers, whereas expression of pVP2 by itself leads to irregular assemblies (Caston et al., 2001).

The available structural data thus shows that dsRNA and +sRNA icosahedral viruses each have their own characteristic capsid architectures, suggesting that they belong to separate viral lineages. Among dsRNA viruses, it has been proposed that the single-layered totiviruses may have lost the outer layers during evolution and thus have become strictly intracellular. Similarly, the *Birnaviridae* may have lost the characteristic internal capsid during evolution from a *Reoviridae*-like ancestor and concominantly adapted the T = 13 protein to make a tightly sealed shell. Alternatively, the complex *Reoviridae* and *Cystoviridae* may have arisen by combination of gene segments from simpler viruses, like the single-layered toti- and birnaviruses. The results presented in this manuscript are in support of this second view. Indeed, we show that the birnavirus coat protein, VP2, has the same jelly roll fold and an arrangement typical of +sRNA viruses, with an inserted domain that is homologous to that of the projecting domain of the T = 13 protein of the *Reoviridae*. Our results provide direct evidence for close relations between the capsid proteins of +sRNA viruses and those of dsRNA viruses, revealing a clear structural relationship between viruses of these two lineages.

Results

The VP2 Trimer

The details of the crystals and the structure determination are provided in Experimental Procedures. The VP2 subunit is folded into three distinct domains disposed radially in the SVP. They are labeled base (B), shell (S), and projection (P), as indicated in Figure 1. The sequence alignment shows that domains S and B are relatively well conserved but that domain P is more variable. The S domain is central to the organization of the molecule, with domain P inserted in a loop between two S domain β strands and domain B formed by α helices from N- and C-terminal extensions of the polypeptide chain, as shown color-coded in the ribbons and topology diagrams. Both domains S and P are β barrels with the jelly roll topology, oriented such that the β strands are tangential and radial, respectively, to the spherical particle. The S_{BIDG} β sheet (S domain) faces domain B, and the corresponding P_{BIDG} sheet (in domain P) is involved in inter subunit contacts in the trimer. Domain S has a wedge-like shape similar to jelly-roll domains observed in capsid proteins from +sRNA viruses. It has an additional β hairpin, C′C″, making the outward facing β sheet six-stranded, ($S_{C''C'CHEF}$).

As shown in Figure 2A, all three domains of VP2 participate in trimer contacts. The $P_{AA'}$ β hairpin makes a flap that invades and completes the β barrel of the neighboring P domain in the trimer, contributing a fifth antiparallel strand at the edge of each β sheet, as shown in Figures 2A. The $P_{AA'}$ flap is thus an important stabilizing element of the VP2 trimer. The wedge-shaped S domain participates in trimer contacts via the thick end of the barrel, with the bulky loops $S_{CC'}$, $S_{C''D}$, S_{EF}. The thin end (with loops S_{BC}, $S_{C'C''}$, S_{DE}, and S_{FG}) points away from the trimer center, with loop S_{DE} form-

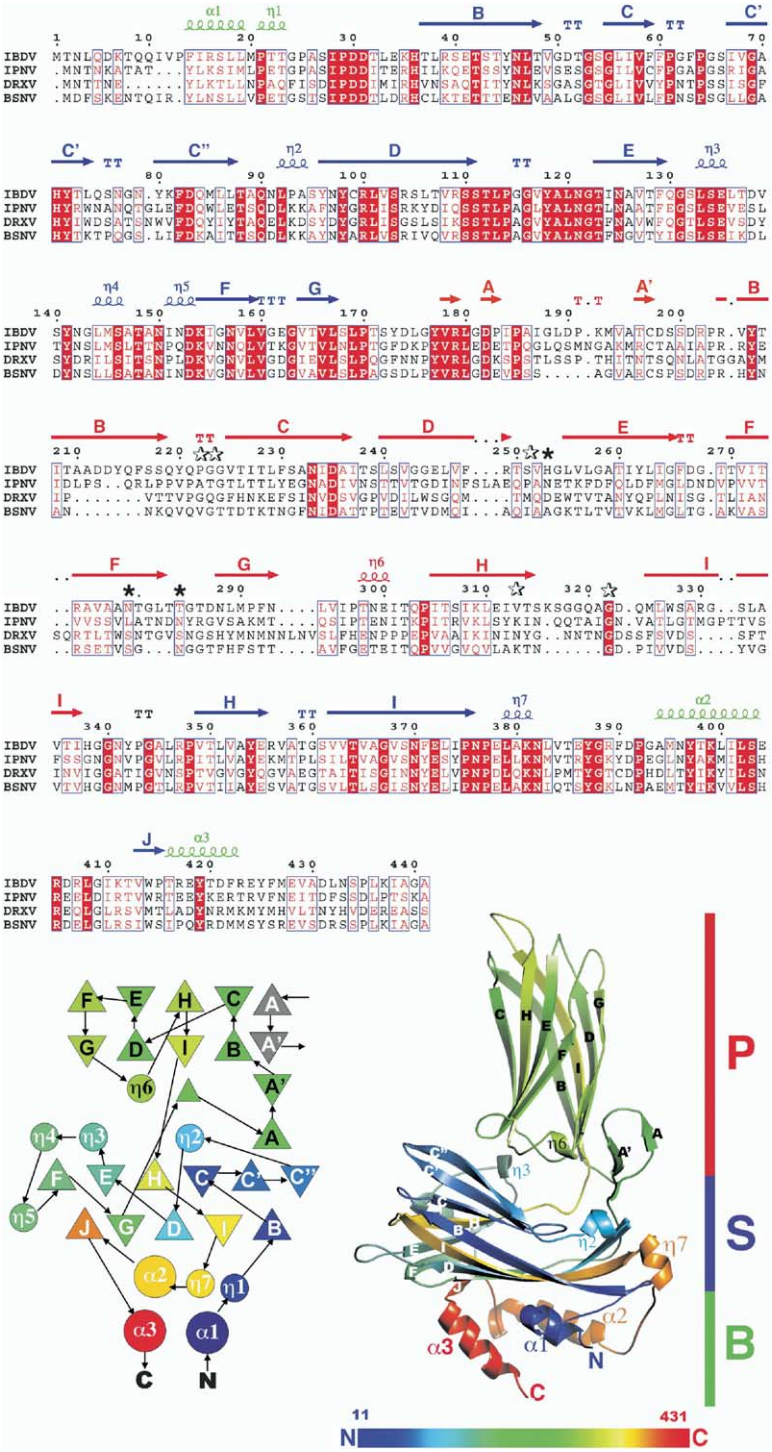

Figure 1. The VP2 Subunit

The top panel displays a sequence alignment of birnavirus VP2 for IBDV (accession number P15480), IPNV (AJ622822), *Drosophila* X Virus (DRXV, U60650), and Blotched Snakehead virus (BSNV, AJ459382). The secondary structure elements are drawn above the IBDV sequence with ESPript (Gouet et al., 2003) and color coded by domain (red, P; blue, S; and green, B, according to the bar to the right of the bottom panel). Strictly conserved residues are white on a red background, and partially conserved residues are red. Solid stars denote residues associated to virulence changes, and open stars mark neutralization-escape mutations (see text). (Bottom left) Topology diagram (program TOPS [Flores et al., 1994] with triangles and circles denoting β strands and helices, respectively; large and small circles indicate α- and 3/10- (labeled η) helices. (Bottom right) Ribbon diagram of VP2. These two panels are colored according to the ramp indicated in the horizontal bar, from blue (N-ter) to red (C-ter). The secondary structure elements of domains S and P are labeled in white and in black, respectively.

ing the vertices of the triangular molecule. Overall, each subunit buries 4700 Å^2 of its surface upon trimer formation. The extent of the contacts strongly suggests that the VP2 trimer is the building block for virus assembly. The crosssection of the trimer in the S domain region has the shape of an equilateral triangle, the side of which is about 100 Å and has about 25 Å in thickness (Figure 2A). This region insures a tight sealing of the virion through extensive lateral contacts in the T = 13 lattice (see below). The overall height of the molecule, including all three domains, is 85 Å.

Determinants of Antigenicity and Virulence

Crossneutralization and crossprotection experiments have revealed two different serotypes of IBDV. The amino acid differences between the two serotypes—and among the pathogenic serotype I isolates—map mainly to domain P, between amino acids 206 and 350.

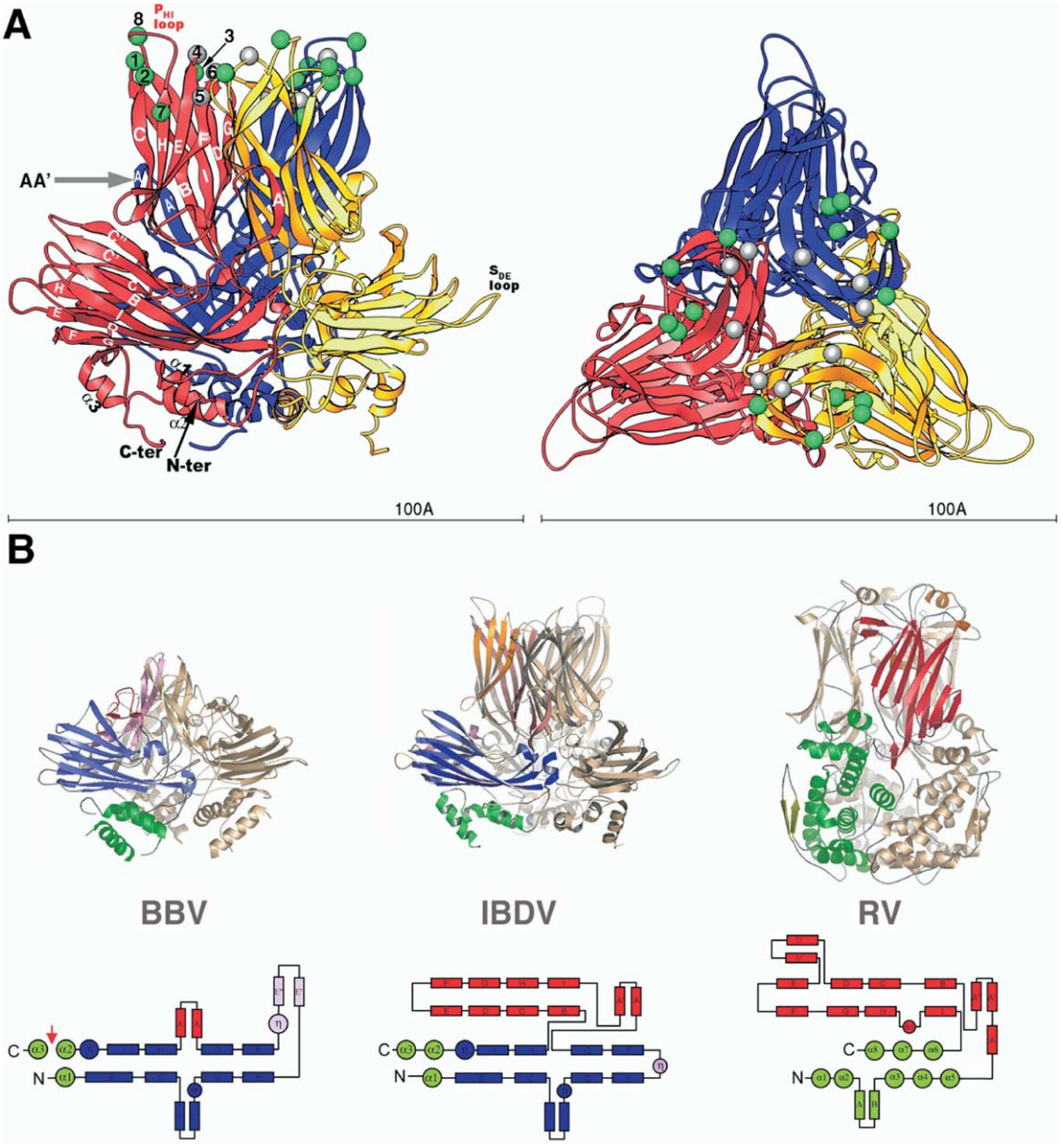

Figure 2. The VP2 Trimer

(A) Ribbon diagram of the VP2 trimer (left, side view; right, top view). Each subunit is colored differently. β strands and α helices are labeled for one subunit in the side view, showing the AA′ β hairpin (indicated by the gray arrow) of domain P embracing the neighboring subunit. Important loops (described in the text) are labeled. Spheres indicate α carbons of residues identified in neutralization escape mutants (green) and cell culture adaptation/virulence changes (gray). The spheres are labeled for the subunit in red: 1, P222; 2, G223; 3, S251; 4, H253; 5, N279; 6, T284; 7, V313; 8,G322. Note the clustering of these amino acids at the top of the spike, with gray spheres at the center and green spheres all around.

(B) The VP2 structure is a link between two different categories of RNA viruses. Ribbon diagrams and simplified topology cartoons (with α helices as circles and β strands as rectangles), color coded by domains, of the capsid proteins of Black Beetle virus (BBV, protein β, PDB code 2bbv), IBDV (protein VP2), and rotavirus (RV, protein VP6, PDB code 1qhd). The DALI score between VP2 and BBV protein β is 15.3, and the rms is 3.3 Å for 211 α carbons (out of 250 residues from domains B and S). The DALI score between VP2 and RV VP6 is 5.1, with 3.5 Å rms for 105 superposed P domain α carbons (out of 140 residues in total).

Furthermore, antibody neutralization-escape mutations point to residues at positions 222 and 223 (loop P_{BC}), 251 (P_{DE}), and 313 and 322 (P_{HI}) (Schnitzler et al., 1993), all in the outmost loops of the P jelly roll, as shown in Figure 2A.

Using reverse-genetics systems, it was shown that IBDV adaptation to cell culture (Lim et al., 1999; Mundt, 1999) and virulence (Brandt et al., 2001; van Loon et al., 2002) are controlled by changes in a few amino acids in VP2 at positions 253 (loop P_{DE}), 279 (strand P_F), and 284 (loop P_{FG}). Figure 2A shows that these positions are located in the most exposed loops of domain P, in

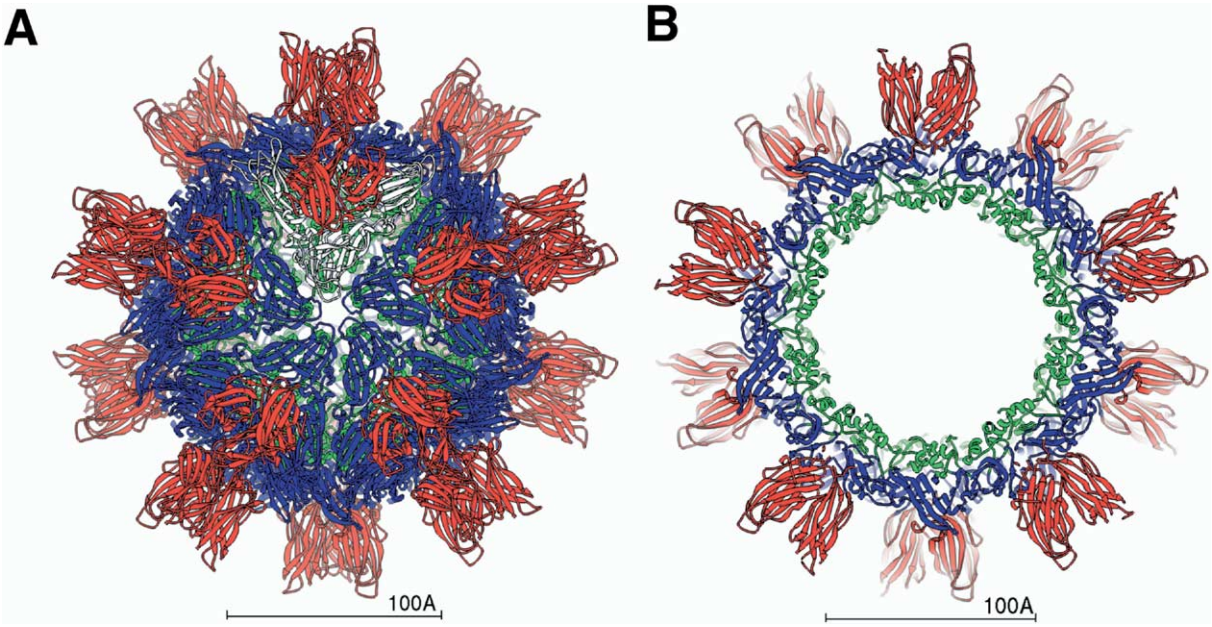

Figure 3. The IBDV Subviral Particle

Ribbon diagram of the SVP, formed by 20 VP2 trimers interacting via I2 and I5 axes. View down the I5 axis.

(A) Full particle, showing the S_{DE} loop closing a channel along the 5-fold axis. One VP2 trimer is highlighted in white for its S domain, with all others following the color scheme defined in Figure 1.

(B) A 60 Å slab of the SVP, containing the center of the particle, showing the concentric distribution of the three domains B, S, and P.

the region of highest antigenic variation. Interestingly, the side chains of H253 and T284 interact via a hydrogen bond, which rigidifies their conformation. All three amino acids implicated in virulence changes have their side chains pointing outward and participate neither in contacts important for the VP2 fold nor in interactions between subunits that stabilize the virion. Their marked effect on virulence thus suggests that these residues may engage directly in contacts with a receptor of the target cell. Note the distribution of the mutations in the trimer in Figure 2A, with the virulence mutations within the central bowl at the top and the antigenic mutations all around.

Structural Homology to Other Viral Capsid Proteins

Domains S and B together display a very high DALI score (Holm and Sander, 1995) with the capsid protein of noda- and tetraviruses, illustrated in Figure 2B, left panel. The coat protein of these T = 3 and T = 4 icosahedral viruses, respectively, include the same C′C″ insertion in the jelly roll and the α-helical N and C-terminal extensions making up domain B. The similarity extends to the quaternary interactions, with the same loops participating in similar trimeric contacts. In contrast, the tertiary and quaternary structure of domain P is most similar to the corresponding domain of orbivirus VP7 (Grimes et al., 1995), rotavirus VP6 (Mathieu et al., 2001), and reovirus μ1 (Liemann et al., 2002), i.e., the proteins forming the T = 13 layer of the *Reoviridae* (illustrated in the right panel of Figure 2C). Moreover, the latter viral proteins, although they lack the S domain, also have an α-helical B domain formed by N- and C-terminal extensions. This domain is, however, more extensive than the B domain of VP2, with several additional α helices.

The IBDV Subviral Particle

Twenty VP2 trimers form the T = 1 SVP, interacting via icosahedral 2-fold (I2) and 5-fold contacts, as illustrated in Figure 3. The area buried per trimer in the SVP is 2500 $Å^2$. Both domains S and B participate in the contacts, forming a continuous 40 Å thick shell with external diameter of 180 Å. Figure 3B shows the concentric organization of the three domains in the particle. The projections formed by domain P are 40 Å long, giving the particle a spiky and pronounced dodecahedral shape, with a total diameter of about 260 Å. As seen in Figure 3A, the interactions between VP2 trimers about the I2 axes involve the edges of the S jelly rolls, using the whole length of the triangular crosssection. The S_{DE} loop (labeled in Figure 2A) reaches the I5 axes and seals a pentameric channel formed underneath by helix α3 and its counterpart from adjacent, I5-related trimers. This channel is depicted in Figure S1 in the Supplemental Data available with this article online along with its counterparts from the T = 13 IBDV virion (described below). As illustrated in Figure S1, a very similar arrangement at the I5 axes has been observed in the virus particle of noda- and tetraviruses (Helgstrand et al., 2004).

The IBDV Virion

The T = 13 icosahedral particle is formed by 260 VP2 trimers, 20 of which lie on icosahedral 3-fold (I3) axes and the others in general positions. Figure 4 displays the 7 Å resolution electron density (ED) map of IBDV

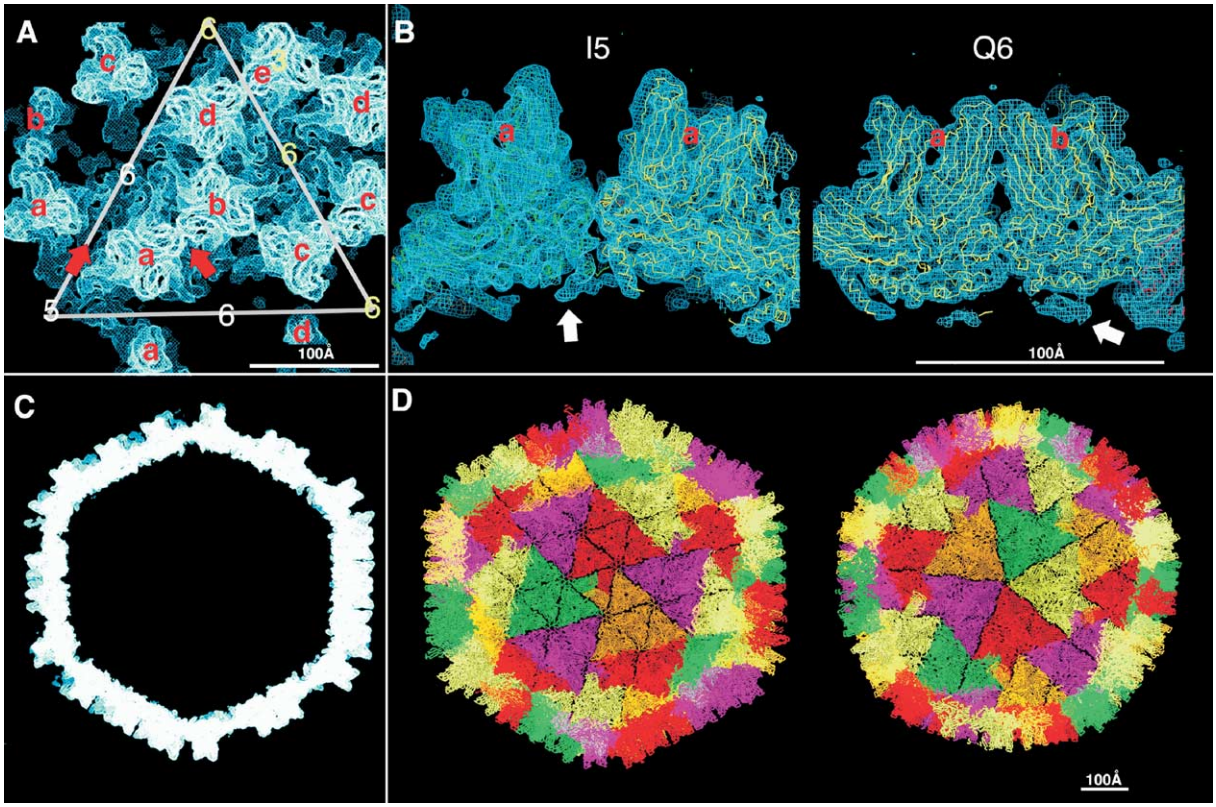

Figure 4. The IBDV Virion

(A) Section of the ED map of the IBDV particle at 7 Å resolution after 60-fold ncs averaging as explained in the Experimental Procedures. The five independent trimers (a–e), defined in Bottcher et al. (1997), are labeled in red. The symmetry axes are labeled in white and in yellow. The icosahedral T = 13 lattice displays two different sets of nonequivalent Q6 axes, one surrounding the I3 (yellow) and the other the I5 axes (white). A gray triangle linking one I5 and two yellow Q6 axes encloses the density corresponding to a G4 triangle described in the text. The flat contact between trimers within a G4 triangle results in head-to-head contacts between P domains. The red arrows point to two extreme types of contacts observed between VP2 trimers, one about the 5-fold and one within a G4 triangle, enlarged in (B).

(B) Side view of the ED corresponding to the contacts indicated by arrows in (A), labeled accordingly, with the Cα carbon skeleton of VP2 superposed. Regions of additional α-helical density underneath the molecule, corresponding to additional ordered VP2 residues at the N- and C termini, are indicated by arrows.

(C) Vertical 200 Å thick ED slab through the center of the IBDV particle, viewed roughly down the I3 axis. Note the flat faces resulting from the interaction of I3 trimers and G4 triangles (see text).

(D) Half an IBDV particle viewed down the I3 (left) and the I5 (right) axes. Only the Cα carbon skeleton of the VP2 trimers fitted into the ED is displayed. Five different colors (yellow, orange, red, green, and magenta) were used for the 60 icosahedral asymmetric units, distributed such that immediate neighbors are colored differently. A flat face of the icosahedron (perpendicular to the I3) is formed by three colors, with the I3 VP2 trimer at the center (linking three G4). For simplicity, the front half of the virion has been removed, showing the concave internal face of the particle. I3 and I5 are located where three and five colors meet, respectively.

with the fitted 3 Å model of the VP2 trimer. The packing of VP2 at the virus surface fully exploits the geometry of the equilateral triangular crosssection of the trimer. Groups of four (G4) VP2 trimers (Figure 4A) associate roughly in a plane to make a bigger equilateral triangle (labeled "G4 triangle") to cover four times the area of a VP2 trimer. In the T = 13 lattice, VP2 trimers lying on the I3 axes, termed "I3 trimers," bridge three G4 triangles to make the 20 flat faces of the icosahedral particle (Figure 4D). The contacts between VP2 trimers within a G4 triangle, as well as those made by the I3 trimer, are all quasiequivalent. In addition to the lateral B-B and S-S domain interactions, they involve head-to-head contacts made by domain P (Figures 4A and 4B). The stronger curvature imposed at the I5 axes forces a different, broken, SVP-like type of contacts between G4 units. The final arrangement is such that there are 20 flat faces made of 13 VP2 trimers (three G4 triangles surrounding a central I3 trimer), resulting in a closed particle with a markedly polyhedral shape.

Two Alternative Conformations of the S_{DE} Loop

VP2 remains essentially unchanged in the virion with respect to the observed conformation in the SVP. The only visible differences at 7 Å resolution are in the S_{DE} loop and in helices α1 and α3 of domain B. There is density for additional ordered amino acids at the VP2 N- and C termini (Table 1 and Figures 4, 5, and S1). The pattern of α helices at the I5 is similar to that of the SVP (Figure S1), while a broader 6-helix channel is observed at the Q6 axes, as shown in Figure 5. Above the Q6 channel, the conserved S_{DE} loop adopts two alternative conformations (up and down, or U and D in

Table 1. Crystallography Statistics

Characteristics of the Crystals						
Crystal	Space group	Cell parameters (Å)	Diffraction limit	Resolution limit (data collection)	Number of ncs operations	MDa in crystallographic asymmetric unit
IBDV SVP form I	$P6_322$	a = 261.0; c = 353.1	4 Å	4 Å	10	0.48
IBDV SVP form II	$P6_3$	a = 258.9; c = 347.2	3 Å	3 Å	20	0.96
IBDV SVP form III	P23	a = 326.1	6 Å	6 Å	10	0.48
IPNV SVP	I23	a = 303.2	3.4 Å	3.4 Å	5	0.24
IBDV virion	$P2_1$	a = 854.0; b = 692.2; c = 792.4; β = 90.0 deg	approaching 4 Å	7 Å	60	37.9
IBDV SVP Form II Crystals; Data Collection Statistics						
Resolution limits			40–3.0 Å			
Completeness			97.2% (91%)			
Signal/noise ratio			11 (2.6)			
R_{sym}			12.5% (43%)			
Molecular Replacement Statistics						
$R_F/CC/R_I$[a] (10–4 Å)			22.0%/46.4%/28.8%			
Refinement Statistics (between 10 and 3 Å Resolution, IBDV-SVP Crystal Form II)						
Number of reflections of working set (test set)			251175 (7361)			
Number of protein atoms/water molecules			20 × 3209/20 × 47			
RMSD of bond lengths/bond angle/main chain B			0.008 Å/1.54°/1.412 Å^2			
Refined twin fraction			17%			
R/R_{free}[b]			21.5%/24.9%			
IBDV Virion Crystals; Data Collection and ncs Averaging Statistics						
Resolution (Å)	R_{sym}	Number of reflections	Completeness (%)	I/sigma	R_{factor}[c]	Correlation coefficient[c]
50–11.08	0.092	312663	85.9	11.58	0.146	0.948
11.08–8.81	0.132	288182	79.5	7.22	0.168	0.928
8.81–7.70	0.280	259239	71.6	2.92	0.227	0.878
7.70–7.00	0.466	229566	63.4	1.72	0.299	0.717
Overall	0.144	1089650	75.1	5.68	0.200	0.922
Molecular Replacement Statistics of Pseudoatomic Model into IBDV Crystals						
$R_F/CC/R_I$[a] (50–15 Å)			43.0%/50.0%/38.0%			
VP2 Model: Amino Acids with Ordered Density in the Different Crystals						
SVP IBDV (form II)[d]			11–431			
IBDV T = 13 particle crystals[e]			Trimer	Chain A	Chain B	Chain C
			a	13–437	1–436 (I5 axis)	12–434
			b	12–441	12–437	13–428
			c	12–441	13–435	13–441
			d	13–436	12–428	13–441
			e	13–441 (I3 axis)		

[a] R_F and CC are the R_{factor} and correlation coefficients (respectively) between calculated (F_c) and observed (F_o) structure factor amplitudes, and R_I the R_{factor} between calculated and observed intensities.
[b] The free set contained 3% of the reflections and was selected using all reflections within thin resolution shells to avoid bias from ncs and twin-operator relations between reflections from the same shell.
[c] The F_c used for these R_{factor} and correlation coefficient was calculated from the 60-fold averaged ED map.
[d] All chains were considered identical in the crystallographic asymmetric unit, obtained by averaging 20 times about ncs axes.
[e] Thirteen independent subunits were considered, distributed in five different trimers labeled a–e (Figure 4A). Only one subunit in trimer e is independent, since this trimer lies on the I3 axis. Chain B in trimer a is also unique because it projects toward the I5 axis, all the other subunits projecting toward Q6 axes.

Figure 5B). These two conformations intercalate and form two sets of pseudo-3-fold contacts about the Q6 axes at different radii (inner for D and outer for U, Figure 5D), resulting in a tighter seal than at the I5 axes.

Discussion

The most important discovery stemming from these structures is that the birnavirus coat protein is formed by domains that are homologous to the coat proteins of both +sRNA and dsRNA viruses. These two viral lineages have each their own characteristic icosahedral architecture, and this is the first time that a structural relationship between them is established. The observed homology to the T = 13 protein of the *Reoviridae* could have been anticipated, since the EM reconstructions show similar trimeric projections at low resolution, and the triangulation of the surface lattice is the same.

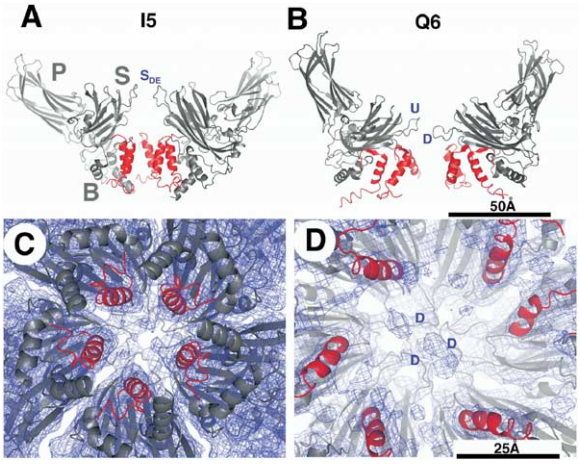

Figure 5. VP2 Interactions about I5 and Q6 Axes

Organization of the α3 helix and the S_{DE} loop in the T = 13 lattice. (A and B) Side views of the I5 and Q6 VP2 arrangements, respectively, with the symmetry axis vertical in the plane of the figure. For simplicity, only one subunit (in gray) from two of the trimers participating in the contact (5 in [A] and 6 in [B]) is shown. The α3 helices of all the subunits participating in the contact are depicted in red. The three domains of VP2 and the loop projecting toward the I5 are labeled in (A). In (B), the two alternative up/down (U and D) conformations of the S_{DE} loop about the Q6 axis are indicated (see text).

(C and D) View down the respective symmetry axis, looking from inside the virion, down the gray arrows of (A) and (B). The ring of five helices shown in (A) and (C) is similar to that observed in the capsid of noda- and tetraviruses (see Supplemental Data). In (B), the three S_{DE} loops in the D conformation, forming the inner 3-fold contact, are labeled. The other three loops interact similarly at a higher radius (not visible in this view). In (D), notice the presence of some noninterpreted density features in the foreground.

Additional information provided by the IBDV structure is that, contrary to a previous report (Ozel and Gelderblom, 1985), the hand of the birnavirus surface lattice is the same as the T = 13 *laevo* lattice of the *Reoviridae*. This finding establishes an additional level of similarity between these two virus families, suggesting conservation of the overall pattern of contacts between trimers at the particle surface. In contrast, the homology to the noda- and tetraviruses was unexpected and raises important questions about their possible evolutionary links with birnaviruses. Interestingly, it has been shown that certain T = 3 fish nodaviruses have a coat protein in which an inserted domain forms trimeric projections (Tang et al., 2002) very similar to those of birnavirus VP2. It is now important to obtain more detailed information on the fold of their coat protein, since it would provide valuable information to understand the links between the two families.

An additional similarity with noda- and tetraviruses is the organization of their bisegmented genomes (Hanzlik and Gordon, 1997; Schneemann et al., 1998), one RNA segment coding for the polymerase and the other for the capsid protein, the latter undergoing proteolytical maturation in both cases. The mRNAs, like the birnavirus mRNAs, are also nonpolyadenylated. The birnavirus Vpg-linked genome replication strategy (Delmas et al., 2004), which has been observed elsewhere only in a subset of +sRNA viruses, including picornaviruses (Paul et al., 1998), is a further common feature bringing birnaviruses and +sRNA viruses together. Finally, some +sRNA ("tetra-like") viruses share with birnaviruses a characteristic polymerase motif rearrangement (Gorbalenya et al., 2002) not found in other viruses. Similarities between replication enzymes do not necessarily match similarities between the corresponding virus capsid architecture (DeFilippis and Villarreal, 2001), but here is a compelling case in which both the capsid proteins and the replication enzymes are clearly related, suggesting homology of the corresponding genes and probably relationships among the entire genomes.

Organization of the Virus Capsid

How is the T = 13 layer formed? VP2 spontaneously forms small SVPs, suggesting that the reason for late maturation is to avoid such premature assembly during particle morphogenesis. Furthermore, it has been experimentally shown that VP3 (a protein of 253 amino acids) interacts with the C-terminal segment of the VP2 precursor, pVP2, and with VP1, thus also controlling polymerase and genome incorporation into the nascent particle. The VP2 C terminus is found very near the 5-fold axes, and it is possible that the presence of the bulky C terminus of pVP2 interferes with 5-fold contacts, which would therefore only take place upon maturation.

Whatever the actual assembly pathway, something must control the association of the 13 trimers present at each of the 20 flat faces of the particle, preventing the extension into 2D arrays. VP3 thus seems to play a key role in assembly. The experimental ED map shows, however, that the strictly ordered part of the IBDV coat is made exclusively by VP2, in contrast to a previous interpretation at lower resolution (Bottcher et al., 1997). This is in spite of the fact that VP3 is definitely present in the crystals in a VP2/VP3 ratio of roughly 1:1, as analyzed by SDS-PAGE and Coomassie blue staining (data not shown). The only additional density observed after extensive 60-fold averaging, using a solid-angle mask including the interior of the particle (see Experimental Procedures), could be interpreted in terms of the N- and C-terminal ends of VP2, which are disordered in the SVP. However, caution is required here, since, at 7 Å resolution, it is not possible to completely rule out that part of the extra density is due to the small segments of other polypeptides (to the pVP2-derived peptides or even to VP3). Notwithstanding, this observation means either that VP3 is not organized or that it is arranged differently within the virion. This second alternative is consistent with previous reports on IPNV describing thread-like ribonucleoprotein complexes containing VP3 and the genomic RNA (Hjalmarsson et al., 1999). It is important to point out that different relative amounts of VP3 and VP2 have been reported in virions from different birnavirus species (Dobos et al., 1979).

Our data show that VP2 relies on a transient scaffold provided by inner proteins to reach the observed T = 13 *laevo* architecture of the virion. Similarly, the *Reoviridae* homologs of VP2 can only form such a lattice on top of the inner capsid, which, in this case, acts as a permanent inner scaffold. More structural information is

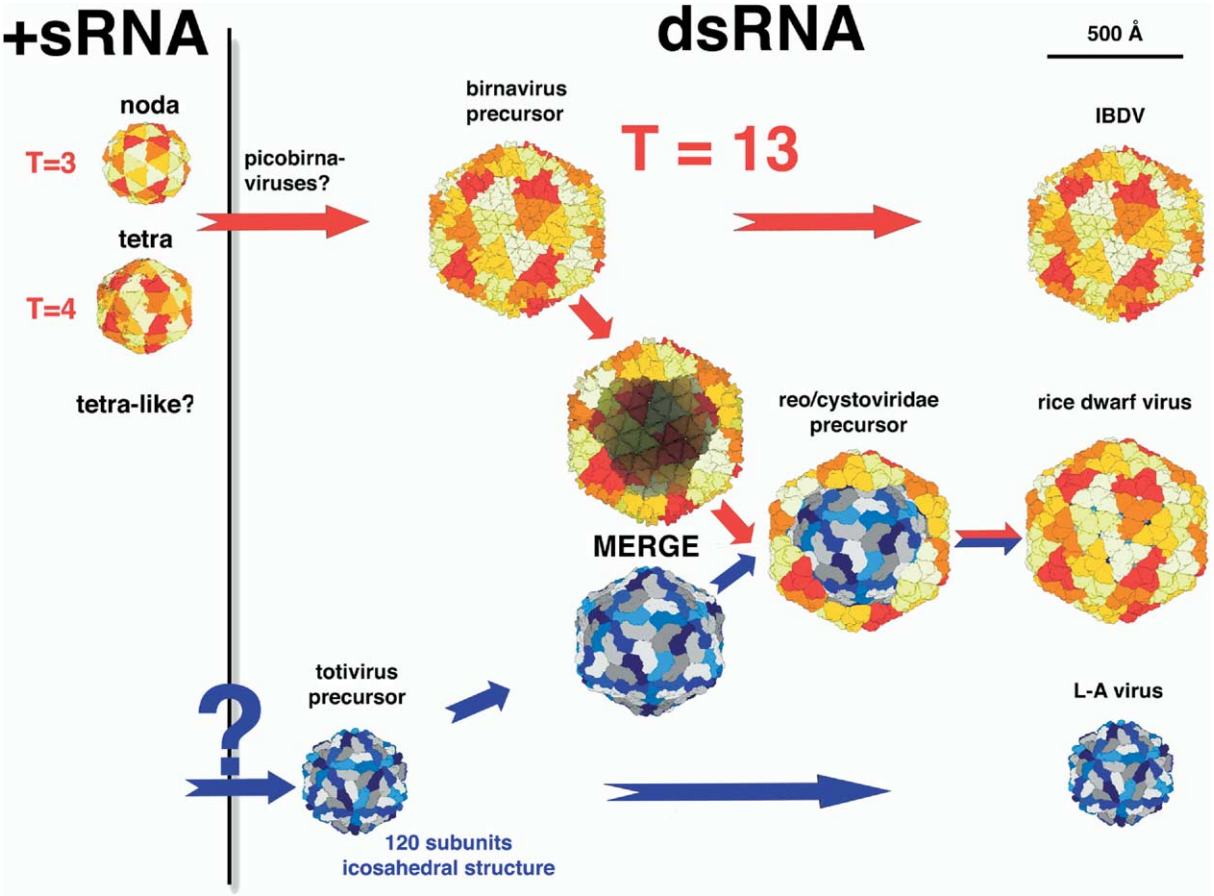

Figure 6. Putative Emergence of the *Reoviridae* by Merging of Genome Segments from Two Simpler dsRNA Viruses

Yellow/red colors represent *Birnaviridae*-related structures and blue/gray colors the *Totiviridae*-related counterparts. The vertical bar indicates a boundary between +sRNA and dsRNA viruses, and time is horizontal (without scale). The top row symbolizes the possible transition from noda- or tetraviruses to IBDV (through a putative T = 13 birnavirus precursor). The bottom row represents the separate emergence of toti-like viruses, perhaps also from +sRNA viruses (because of RdRp similarities). The middle row illustrates the proposed merging of genomic segments that gave rise to a precursor of the more complex, muiltilayered *reo*- and *Cystoviridae*. Drawings made from the coordinates of nodavirus BBV (PDB code 2bbv), tetravirus NωV (PDB code 1ohf), totivirus L-A (PDB code 1m1c), the phytoreovirus RDV (PDB code 1uf2), and IBDV.

needed to determine whether VP3 bears any resemblance to the inner capsid protein of the *Reoviridae*.

Implications for the Capsid Transcriptase Activity

The similarity of the virion organization about the I5 axes with the noda- and tetraviruses, illustrated in Figure S1, is striking. The α-helical hydrophilic channel in all three viruses can easily accommodate a single-stranded RNA molecule. The entry pathway of nonenveloped +sRNA animal viruses is not clearly understood, but this α-helical arrangement has been postulated to be involved in extrusion of the viral genome from the capsid (Munshi et al., 1996). It is possible that the α-helical channel is used for translocating the newly transcribed birnavirus mRNAs across the capsid. Extrusion of mRNAs through pores at the I5 axes has indeed been observed for members of the *Reoviridae* (Diprose et al., 2001; Lawton et al., 1997). As shown in Figure 5, the highly conserved S_{DE} loop seals the I5 channels at the vertices of the particle. Interestingly, this loop is seen to adopt two different conformations at the Q6 axes and could possibly display a concerted switch between two alternative conformations, opening and closing the gate for mRNA translocation at the I5 axes.

In contrast to the *Reoviridae* (Dryden et al., 1998; Gouet et al., 1999), we have observed no additional density suggesting the presence of a transcription complex right under the I5 axes, nor density corresponding to partially ordered dsRNA helices, even at contour levels as low as 0.2 sigma values. The smaller birnavirus genome size—6 kilobase pairs (kbp) compared to the 18–24 kbp genome of the *Reoviridae*—may explain this difference. Accordingly, the buoyant density of the birnavirus particles is 1.33 g/cm^3, compared to 1.43 g/cm^3 and 1.44 g/cm^3 for the reovirus and rotavirus cores, respectively, which enclose a similar volume for a genome three to four times bigger.

Evolutionary Links between +sRNA and dsRNA Viruses

Evolution is a complex process that cannot be described unidirectionally. The birnaviruses that we are seeing today could be remnants of more complex machineries that have lost, for instance, their *Reoviridae*-

like inner and outer layers. It could even be that +sRNA viruses appeared as yet simplified versions of the more complex birnaviruses. However, there are so many similarities between birnaviruses and +sRNA viruses, and at the same time so many differences between the other proteins of the dsRNA viruses in general with +sRNA viruses, to advocate the opposite view. Besides their dsRNA genomes, the only bridging element between birnaviruses with the other dsRNA viruses is the T = 13 protein layer. Indeed, all of the other *Reoviridae* genes seem to be completely unrelated. It is thus possible that a putative intracellular toti-like virus ancestor may have acquired a genomic segment coding for the capsid protein of a birna-like virus, as diagrammed in Figure 6, endowing it with the capability of horizontal transfer between cells and leading to the appearance of a *Reoviridae* (and likely a *Cystoviridae*) ancestor. Within this view, the presence in the new virion of an inner layer ensuring a tight sealing resulted in the loss of the S domain of the T = 13 protein during an adaptation process, since its sealing role became redundant. The loss of the S domain was probably accompanied by an important reorganization of the B domain, which is more extensive and has many more α helices. Indeed, the B domain is much more variable between different members of the *Reoviridae* than is the P domain.

Membrane Translocation

In addition to acquiring a birnavirus-like T = 13 layer surrounding the core, many *Reoviridae* also acquired several other genes for viral entry, including coat proteins that form a third, external layer. In some cases, these new proteins are responsible for membrane penetration, as in rotaviruses, but in others, like the orthoreoviruses, it is the VP2 homolog (protein μl), that is responsible for membrane penetration. In the case of the bluetongue virus, an orbivirus transmitted by insect vectors, particles lacking the outer layer are highly infectious for insect cells (Mertens et al., 1996). This observation implies a role for the T = 13 middle layer protein VP7, which contains an exposed RGD sequence important for interactions with receptors (Tan et al., 2001), in entry. These functional data from the *Reoviridae* homologs strongly support the hypothesis that birnavirus VP2—for which there are currently no experimental data supporting its membrane penetration abilities—may play the same role during entry, especially since it is the only protein available at the viral surface for the relevant interactions with the host. In addition, a role during entry could explain the paradoxical conservation of the P domain between *Birnaviridae* and *Reoviridae*, in spite of the fact that it plays little part in the contacts to form the T = 13 layer and should therefore be less functionally constrained.

Concluding Remarks

Two main conclusions can be drawn from the data reported here. First, the structure of VP2 reveals unexpected relationships among icosahedral viruses of very different categories, shedding light on their possible overall evolutionary pathway. Second, only VP2 is present in the icosahedral shell protecting the birnavirus genome. One single polypeptide—with the possible help of peptides derived from its precursor—must thus carry the functions of several capsid proteins of viruses of the *Reoviridae* family, participating both in membrane translocation and in extrusion of mRNAs during transcription. The structure of the birnavirus particles now opens the way for a rational and concerted approach to dissect and understand the molecular mechanisms put forth by this multifunctional protein during the viral cycle.

Experimental Procedures

Crystallization

SVP

IBDV and IPNV SVPs were produced using a previously published protocol (Chevalier et al., 2002). SVPs were dialyzed into a solution of 50 mM ammonium acetate (pH 7) and concentrated on vivaspin to about 10 mg/ml. Crystals were grown by vapor diffusion using polyethylene glycol as precipitant. The IBDV SVP crystallized in three crystal forms (see Table 1) under the following conditions: form I in 16%–24% PEG 400, 50 mM sodium acetate (pH 5); form II under the same conditions as form I but adding 50–150 mM NaCl; form III in 3%–8% PEG 8000, 100 mM Tris (pH 8). The IPNV SVP crystals grew from 1 M 1,6-hexanediol, 10 mM CoCl2, 100 mM sodium acetate (pH 4.6). For data collection at 100 K, form II crystals were transferred progressively to a cryoprotecting solution containing the same buffer and 28% PEG 400 plus 20% methyl-pentanediol (MPD) before flash cooling.

Viral Particles

Viral suspensions of the vaccine strain CT of IBDV were provided by MERIAL and purified using a CsCl gradient, as described previously (Da Costa et al., 2002). The sample was dialyzed into the same buffer as the SVPs and concentrated roughly to 5 mg/ml. Crystals were obtained by vapor diffusion, with 1.6%–2% PEG 8000, HEPES 100 mM (pH 7.5), and 0.5 M KSCN 20% glycerol and 20% MPD. For data collection, the crystals were flash cooled to 100 K.

Structure Determination

The crystals used for the structure determination, their space group, and diffraction characteristics are listed in Table 1. All diffraction data were collected using synchrotron radiation and processed using the HKL2000 software (Otwinowski and Minor, 1997) and program PROW (Bourgeois, 1999).

Structure of the SVP

An initial 3.8 Å ED map was obtained for the homologous T = 1 SVP of IPNV. This map was calculated by the single isomorphous replacement (SIR) method using a mercury derivative, with program SOLVE (Terwilliger and Berendzen, 1999). The initial SIR phases were refined by 5-fold noncrystallographic symmetry (ncs) averaging with RESOLVE (Terwilliger, 2001). The IPNV SVP structure was later further extended to 3.4 Å and will be published separately. The structure of the IBDV SVP was determined by molecular replacement (MR), using AMoRe (Navaza, 1994) to place the IPNV 3.8 Å map into crystal form II (see Table 1). Twenty-fold ncs averaging with program RAVE (Jones, 1992) was used for phase extension to 3 Å resolution. This procedure yielded a very clear ED map that allowed tracing amino acids 11–431 of VP2 with program O (Jones and Kjeldgaard, 1997) and subsequent refinement of the model using CNS (Brünger et al., 1998).

Structure of the Virus Particle

Pseudoatomic IBDV Model

The atomic model of theVP2 trimer was extracted from the SVP and fitted into the available 3D reconstruction of IBDV (Bottcher et al., 1997) to create a pseudoatomic model of the virus particle, containing 260 VP2 trimers, with program URO (Navaza et al., 2002). The fitting showed that the actual hand corresponded to the mirror image of the available reconstruction, which displayed a T = 13 "*dextro*" lattice according to an early determination of the chirality (Ozel and Gelderblom, 1985). The *laevo* chirality of the T = 13

lattice was confirmed separately by rotary shadowing (J.P., C.C., J.N., B.D., and J. Lepault, submitted).

Crystal Structure Determination

The statistics of the 7 Å data set collected from one single IBDV crystal at 100 K are listed in Table 1. The pseudoatomic model was placed in the crystal by MR and refined as 260 independent rigid bodies, using AMoRe, against the measured structure factor amplitudes. This step allowed the correction of possible magnification errors in the initial cryo-EM map. Initial phases were calculated from the refined pseudoatomic model, and 60-fold ncs averaging was used for density modification and removal of model bias, using RAVE, MAMA, and other programs of the Uppsala suite (Jones, 1992). The mask was derived from the pseudoatomic model and covered 1/60 of the virus particle (a G4 triangle + 1 subunit of the I3 trimer, see text) and was extended inward as a solid angle, leaving out only a sphere of 20 Å radius at the center of the particle.

Illustrations

The ribbon diagrams of Figures 1 and 2B were made with PYMOL (W.L. DeLano, "The PyMOL Molecular Graphics System"; DeLano Scientific LLC, San Carlos, CA, USA; http://www.pymol.org). Figure 4 was made with O (Jones and Kjeldgaard, 1997). Figures 2A, 3, 5, and 6 were prepared with RIBBONS (Carson, 1997).

Supplemental Data

Supplemental Data include one figure and can be found with this article online at http://www.cell.com/cgi/content/full/120/6/761/DC1/.

Acknowledgments

This manuscript is dedicated to the memory of Jean Cohen. We thank F.X. Le Gros (MERIAL, Lyon, France) for the IBDV viral suspensions; R.A. Crowther for the IBDV cryo-EM map; J. Caston and J.L. Carrascosa for the IBDV SVP map; B. McClain for a real-space averaging script; S. Duquerroy and A. Vigouroux for help at different stages of this work; E. Stura for discussion; C. Schulze-Briese and T. Tomikazi for help during data collection; J. Lepault and P. Forterre for comments on the manuscript; and G. Aumont and C. Branlant for support. Diffraction data were collected at the following synchrotrons: SLS (beamline X06SA), Paul Scherrer Institut, Villigen, Switzerland; and ESRF, Grenoble, France. F.A.R. and B.D. acknowledge support from the CNRS and INRA, the SESAME Program of the "Région Ile-de-France," the CNRS programs PCV and "Dynamique et réactivité des assemblages biologiques," the ACI "Microbiologie" from the French MRT, and the EU COST action 839. F.C. was funded by a CNRS BDI fellowship and by an INRA fellowship. C.C. was funded by a French MRT fellowship. J.P. acknowledges fellowships of the EMBO (ALTF 230/2002) and the EU (HPMF-CTF-2002-01805).

Received: July 25, 2004
Revised: November 12, 2004
Accepted: January 7, 2005
Published: March 24, 2005

References

Bamford, D.H., Burnett, R.M., and Stuart, D.I. (2002). Evolution of viral structure. Theor. Popul. Biol. *61*, 461–470.

Birghan, C., Mundt, E., and Gorbalenya, A.E. (2000). A non-canonical lon proteinase lacking the ATPase domain employs the ser-Lys catalytic dyad to exercise broad control over the life cycle of a double-stranded RNA virus. EMBO J. *19*, 114–123.

Bottcher, B., Kiselev, N.A., Stel'Mashchuk, V.Y., Perevozchikova, N.A., Borisov, A.V., and Crowther, R.A. (1997). Three-dimensional structure of IBDV determined by electron cryomicroscopy. J. Virol. *71*, 325–330.

Bourgeois, D. (1999). New processing tools for weak and/or spatially overlapped macromolecular diffraction patterns. Acta Crystallogr. D Biol. Crystallogr. *55*, 1733–1741.

Brandt, M., Yao, K., Liu, M., Heckert, R.A., and Vakharia, V.N. (2001). Molecular determinants of virulence, cell tropism, and pathogenic phenotype of IBDV. J. Virol. *75*, 11974–11982.

Brünger, A.T., Adams, P.D., Clore, G.M., DeLano, W.L., Gros, P., Grosse-Kunstleve, R.W., Jiang, J.S., Kuszewski, J., Nilges, M., Pannu, N.S., et al. (1998). Crystallography & NMR system: A new software suite for macromolecular structure determination. Acta Crystallogr. *D54*, 905–921.

Butcher, S.J., Dokland, T., Ojala, P.M., Bamford, D.H., and Fuller, S.D. (1997). Intermediates in the assembly pathway of the double-stranded RNA virus phi6. EMBO J. *16*, 4477–4487.

Carson, M. (1997). Ribbons. Methods Enzymol. *277*, 493–505.

Caspar, D.L.D., and Klug, A. (1962). Physical principle in the construction of regular viruses. Cold Spring Harb. Symp. Quant. Biol. *27*, 1–24.

Caston, J.R., Trus, B.L., Booy, F.P., Wickner, R.B., Wall, J.S., and Steven, A.C. (1997). Structure of L-A virus: a specialized compartment for the transcription and replication of double-stranded RNA. J. Cell Biol. *138*, 975–985.

Caston, J.R., Martinez-Torrecuadrada, J.L., Maraver, A., Lombardo, E., Rodriguez, J.F., Casal, J.I., and Carrascosa, J.L. (2001). C terminus of IBDV major capsid protein VP2 is involved in definition of the T number for capsid assembly. J. Virol. *75*, 10815–10828.

Chevalier, C., Lepault, J., Erk, I., Da Costa, B., and Delmas, B. (2002). The maturation process of pVP2 requires assembly of IBDV capsids. J. Virol. *76*, 2384–2392.

Chevalier, C., Lepault, J., Da Costa, B., and Delmas, B. (2004). The last C-terminal residue of VP3, glutamic acid *257*, controls capsid assembly of IBDV. J. Virol. *78*, 3296–3303.

Cohen, J. (1975). Ribonucleic acid polymerase activity in purified IPNV of trout. Biochem. Biophys. Res. Commun. *62*, 689–695.

Da Costa, B., Chevalier, C., Henry, C., Huet, J.C., Petit, S., Lepault, J., Boot, H., and Delmas, B. (2002). The capsid of IBDV contains several small peptides arising from the maturation process of pVP2. J. Virol. *76*, 2393–2402.

DeFilippis, V.R., and Villarreal, L.P. (2001). Virus evolution. In Fields Virology, D.M. Knipe and P.M. Howley, eds. (Philadelphia: Lippincott-Raven Publishers), pp. 353–370.

Delmas, B., Kibenge, F.S.B., Leong, J.C., Mundt, E., Vakharia, V.N., and Wu, J.L. (2004). Birnaviridae. In Virus Taxonomy, C.M. Fauquet, M.A. Mayo, J. Maniloff, U. Desselberger, and A.L. Ball, eds. (London: Academic Press), pp. 561–569.

Diprose, J.M., Burroughs, J.N., Sutton, G.C., Goldsmith, A., Gouet, P., Malby, R., Overton, I., Zientara, S., Mertens, P.P., Stuart, D.I., and Grimes, J.M. (2001). Translocation portals for the substrates and products of a viral transcription complex: the bluetongue virus core. EMBO J. *20*, 7229–7239.

Dobos, P., Hill, B.J., Hallett, R., Kells, D.T., Becht, H., and Teninges, D. (1979). Biophysical and biochemical characterization of five animal viruses with bisegmented dsRNA genomes. J. Virol. *32*, 593–605.

Dryden, K.A., Farsetta, D.L., Wang, G., Keegan, J.M., Fields, B.N., Baker, T.S., and Nibert, M.L. (1998). Internal/structures containing transcriptase-related proteins in top component particles of mammalian orthoreovirus. Virology *245*, 33–46.

Estes, M.K. (2001). Rotaviruses and their replication. In Fields Virology, D.M. Knipe and P.M. Howley, eds. (Philadelphia: Lippincott-Raven Publishers), pp. 1747–1833.

Flores, T.P., Moss, D.S., and Thornton, J.M. (1994). An algorithm for automatically generating protein topology cartoons. Protein Eng. *7*, 31–37.

Gorbalenya, A.E., Pringle, F.M., Zeddam, J.L., Luke, B.T., Cameron, C.E., Kalmakoff, J., Hanzlik, T.N., Gordon, K.H., and Ward, V.K. (2002). The palm subdomain-based active site is internally permuted in viral RNA-dependent RNA polymerases of an ancient lineage. J. Mol. Biol. *324*, 47–62.

Gouet, P., Diprose, J.M., Grimes, J.M., Malby, R., Burroughs, J.N., Zientara, S., Stuart, D.I., and Mertens, P.P. (1999). The highly or-

dered double-stranded RNA genome of bluetongue virus revealed by crystallography. Cell *97*, 481–490.

Gouet, P., Robert, X., and Courcelle, E. (2003). ESPript/ENDscript: Extracting and rendering sequence and 3D information from atomic structures of proteins. Nucleic Acids Res. *31*, 3320–3323.

Grimes, J., Basak, A.K., Roy, P., and Stuart, D. (1995). The crystal structure of bluetongue virus VP7. Nature *373*, 167–170.

Grimes, J.M., Burroughs, J.N., Gouet, P., Diprose, J.M., Malby, R., Zientara, S., Mertens, P.P., and Stuart, D.I. (1998). The atomic structure of the bluetongue virus core. Nature *395*, 470–478.

Hanzlik, T.N., and Gordon, K.H. (1997). The Tetraviridae. Adv. Virus Res. *48*, 101–168.

Harrison, S.C. (2001a). The familiar and the unexpected in structures of icosahedral viruses. Curr. Opin. Struct. Biol. *11*, 195–199.

Harrison, S.C. (2001b). Principles of virus structure. In Fields Virology, D.M. Knipe and P.M. Howley, eds. (Philadelphia: Lippincott-Raven Publishers), pp. 53–85.

Helgstrand, C., Munshi, S., Johnson, J.E., and Liljas, L. (2004). The refined structure of NwV reveals control elements for a T = 4 capsid maturation. Virology *318*, 192–203.

Hjalmarsson, A., Carlemalm, E., and Everitt, E. (1999). IPNV: identification of a VP3-containing ribonucleoprotein core structure and evidence for O-linked glycosylation of the capsid protein VP2. J. Virol. *73*, 3484–3490.

Holm, L., and Sander, C. (1995). Dali: a network tool for protein structure comparison. Trends Biochem. Sci. *20*, 478–480.

Johnson, J.E., and Speir, J.A. (1997). Quasi-equivalent viruses: a paradigm for protein assemblies. J. Mol. Biol. *269*, 665–675.

Jones, T.A. (1992). A, yaap, asap, @*? A set of averaging programs. In Molecular Replacement, E.J. Dodson, S. Gover, and W. Wolf, eds. (Warrington, England: SERC Daresbury Laboratory), pp. 91–105.

Jones, T.A., and Kjeldgaard, M. (1997). Electron density map interpretation. In Macromolecular Crystallography, Part B, C.W. Carter and R.M. Sweet, eds. (London: Academic Press), pp. 173–208.

Lawton, J.A., Estes, M.K., and Prasad, B.V. (1997). Three-dimensional visualization of mRNA release from actively transcribing rotavirus particles. Nat. Struct. Biol. *4*, 118–121.

Liemann, S., Chandran, K., Baker, T.S., Nibert, M.L., and Harrison, S.C. (2002). Structure of the reovirus membrane-penetration protein, Mu1, in a complex with is protector protein, Sigma3. Cell *108*, 283–295.

Lim, B.L., Cao, Y., Yu, T., and Mo, C.W. (1999). Adaptation of very virulent IBDV to chicken embryonic fibroblasts by site-directed mutagenesis of residues 279 and 284 of viral coat protein VP2. J. Virol. *73*, 2854–2862.

Mathieu, M., Petitpas, I., Navaza, J., Lepault, J., Kohli, E., Pothier, P., Prasad, B.V., Cohen, J., and Rey, F.A. (2001). Atomic structure of the major capsid protein of rotavirus: implications for the architecture of the virion. EMBO J. *20*, 1485–1497.

Mertens, P.P., Burroughs, J.N., Walton, A., Wellby, M.P., Fu, H., O'Hara, R.S., Brookes, S.M., and Mellor, P.S. (1996). Enhanced infectivity of modified bluetongue virus particles for two insect cell lines and for two Culicoides vector species. Virology *217*, 582–593.

Muller, H., Islam, M.R., and Raue, R. (2003). Research on infectious bursal disease—the past, the present and the future. Vet. Microbiol. *97*, 153–165.

Mundt, E. (1999). Tissue culture infectivity of different strains of IBDV is determined by distinct amino acids in VP2. J. Gen. Virol. *80*, 2067–2076.

Munshi, S., Liljas, L., Cavarelli, J., Bomu, W., McKinney, B., Reddy, V., and Johnson, J.E. (1996). The 2.8 Å structure of a T = 4 animal virus and its implications for membrane translocation of RNA. J. Mol. Biol. *261*, 1–10.

Naitow, H., Tang, J., Canady, M., Wickner, R.B., and Johnson, J.E. (2002). L-A virus at 3.4 Å resolution reveals particle architecture and mRNA decapping mechanism. Nat. Struct. Biol. *9*, 725–728.

Nakagawa, A., Miyazaki, N., Taka, J., Naitow, H., Ogawa, A., Fujimoto, Z., Mizuno, H., Higashi, T., Watanabe, Y., Omura, T., et al. (2003). The atomic structure of rice dwarf virus reveals the self-assembly mechanism of component proteins. Structure (Camb.) *11*, 1227–1238.

Navaza, J. (1994). AMoRe: An automated package for molecular replacement. Acta Crystallogr. A *50*, 157–163.

Navaza, J., Lepault, J., Rey, F.A., Alvarez-Rua, C., and Borge, J. (2002). On the fitting of model electron densities into EM reconstructions: a reciprocal-space formulation. Acta Crystallogr. D Biol. Crystallogr. *58*, 1820–1825.

Nibert, M.L., and Schiff, L.A. (2001). Reoviruses and their replication. In Fields Virology, D.M. Knipe and P.M. Howley, eds. (Philadelphia: Lippincott-Raven Publishers), pp. 1679–1728.

Ona, A., Luque, D., Abaitua, F., Maraver, A., Caston, J.R., and Rodriguez, J.F. (2004). The C-terminal domain of the pVP2 precursor is essential for the interaction between VP2 and VP3, the capsid polypeptides of IBDV. Virology *322*, 135–142.

Otwinowski, Z., and Minor, W. (1997). Processing of X-ray diffraction data collected in oscillation mode. In Macromolecular Crystallography, Part A, C.W. Carter and R.M. Sweet, eds. (London: Academic Press), pp. 307–326.

Ozel, M., and Gelderblom, H. (1985). Capsid symmetry of viruses of the proposed Birnavirus group. Arch. Virol. *84*, 149–161.

Paul, A.V., van Boom, J.H., Filippov, D., and Wimmer, E. (1998). Protein-primed RNA synthesis by purified poliovirus RNA polymerase. Nature *393*, 280–284.

Reinisch, K.M., Nibert, M.L., and Harrison, S.C. (2000). Structure of the reovirus core at 3.6 Å resolution. Nature *404*, 960–967.

Rossmann, M.G., and Johnson, J.E. (1989). Icosahedral RNA virus structure. Annu. Rev. Biochem. *58*, 533–573.

Roy, P. (2001). Orbiviruses. In Fields Virology, D.M. Knipe and P.M. Howley, eds. (Philadelphia: Lippincott-Raven Publishers), pp. 1835–1869.

Schneemann, A., Reddy, V., and Johnson, J.E. (1998). The structure and function of nodavirus particles: a paradigm for understanding chemical biology. Adv. Virus Res. *50*, 381–446.

Schnitzler, D., Bernstein, F., Muller, H., and Becht, H. (1993). The genetic basis for the antigenicity of the VP2 protein of the IBDV. J. Gen. Virol. *74*, 1563–1571.

Spies, U., Muller, H., and Becht, H. (1987). Properties of RNA polymerase activity associated with IBDV and characterization of its reaction products. Virus Res. *8*, 127–140.

Tan, B.H., Nason, E., Staeuber, N., Jiang, W., Monastryrskaya, K., and Roy, P. (2001). RGD tripeptide of bluetongue virus VP7 protein is responsible for core attachment to Culicoides cells. J. Virol. *75*, 3937–3947.

Tang, L., Lin, C.S., Krishna, N.K., Yeager, M., Schneemann, A., and Johnson, J.E. (2002). Virus-like particles of a fish nodavirus display a capsid subunit domain organization different from that of insect nodaviruses. J. Virol. *76*, 6370–6375.

Terwilliger, T.C. (2001). Maximum-likelihood density modification using pattern recognition of structural motifs. Acta Crystallogr. *D57*, 1755–1762.

Terwilliger, T.C., and Berendzen, J. (1999). Automated MAD and MIR structure solution. Acta Crystallogr. *D55*, 849–861.

van Loon, A.A., de Haas, N., Zeyda, I., and Mundt, E. (2002). Alteration of amino acids in VP2 of very virulent IBDV results in tissue culture adaptation and attenuation in chickens. J. Gen. Virol. *83*, 121–129.

Accession Numbers

The atomic coordinates and structure factors of the T = 1 and T = 13 IBDV particles have been deposited in the Protein Data Bank under ID codes 1WCD and 1WCE, respectively.